Journal of Genetics (2023)102:50
https://doi.org/10.1007/s12041-023-01447-5

RESEARCH ARTICLE

The formate dehydrogenase enhances aluminum tolerance of tobacco

YONGHONG XIE, YUNMIN WEI, RONGRONG HAN, SHITIAN YU, HUI XU, CAODE JIANG and YONGXIONG YU*

College of Animal Science and Technology, Southwest University, Chongqing 400715, People's Republic of China
*For correspondence. E-mail: yuyongxiong8@126.com.

Received 1 June 2023; revised 17 August 2023; accepted 22 August 2023

Abstract. The formate dehydrogenase (FDH) is regarded as a universal stress protein involved in various plant abiotic stress responses. This study aims to ascertain GmFDH function in conferring tolerance to aluminum (Al) stress. The bioinformatics analysis demonstrates that *GmFDH* from Tamba black soybean (TBS) encodes FDH. Quantitative reverse transcription-PCR (qRT-PCR) showed that *GmFDH* expression was induced by Al stress with a concentration-time-specific pattern. Moreover, Al stress promotes formate content and activates FDH activity. Further studies revealed that *GmFDH* overexpression alleviated root growth of tobacco under Al stress inhibition and reduced Al and ROS accumulation in roots. In addition, transgenic tobacco had much more root citrate exudation and much higher activity of antioxidant enzymes than wild type. Moreover, under Al stress, *NtMATE* and *NtALS3* expression showed no changes in wild type and overexpression lines, suggesting that here the known Al-resistant mechanisms are not involved. However citrate synthase activity is higher in transgenic tobaccos than that of wild type, which might be the reason for citrate secretion increase. Thus, the increased Al tolerance of *GmFDH* overexpression lines is likely attributable to enhanced activities of antioxidant enzymes and promoting citrate secretion. Taken together, our findings advance understanding of higher plant Al toxicity mechanisms and suggest a possible new route towards the improvement of plant growth under Al stress.

Keywords. tamba black soybean; formate dehydrogenase; aluminum tolerance; tobacco.

Introduction

Tamba black soybean (TBS), a leguminous plant like alfalfa, is suitable for growing in acidic soil. The important mechanism of TBS resistance to aluminum (Al) toxicity involves the secretion of citrate from the root tip and chelates Al^{3+} in the rhizosphere under Al stress. Al toxicity is a significant limitation to plant growth and development in acidic soil, accounting for ~50% of the world's arable land (Kochian *et al*. 2015). Moreover, industrial pollution and modern farming practices increase the range and impact of Al toxicity (Eekhout *et al*. 2017). In acidic soil at pH < 5, Al can be released as soluble Al^{3+}, which inhibits the growth of roots, represses the uptake of water and nutrients, and ultimately results in severe loss of plant yield (Zhang *et al*. 2019). To cope with Al stress, Al-tolerant plants have evolved complex mechanisms, which mainly include an external exclusion mechanism and an internal tolerance mechanism (He *et al*. 2019; Muhammad *et al*. 2019). The Al external exclusion mechanism mainly involves the secretion of organic acids (OAs) into the rhizosphere, which can effectively chelate and prevent Al^{3+} from entering the root tip (An *et al*. 2014; Riaz *et al*. 2018; Yang *et al*. 2019). Internal tolerance mechanisms involve Al entering the cytoplasm through the Al transporter on the plasma membrane, where it is chelated by organic acids and phenols, and partially accumulates in vacuoles (Yokosho *et al*. 2016; Lei *et al*. 2017).

Formate dehydrogenase (FDH) is a mitochondrial enzyme found in the mitochondrial matrix, widely distributed in living organisms, and plays a vital role in the metabolism of higher plants under several environmental stress conditions (Ambard-Bretteville *et al*. 2003). Previous studies have reported that FDHs are involved in providing energy and have a pivotal role in maintaining a reducing environment

Yonghong Xie and Yunmin Wei contributed equally to this work.

Supplementary Information: The online version contains supplementary material available at https://doi.org/10.1007/s12041-023-01447-5.

Published online: 11 October 2023

for combatting oxidative stress (Kurt-Gür *et al*. 2018). However, it is noteworthy that formate is released as a critical byproduct during reactive oxygen species (ROS) scavenging (Thomas *et al*. 2016). Moreover, FDH expression was significantly induced by abiotic stress conditions such as drought, heavy metal pollution, temperature changes, and pathogens (Andreadeli *et al*. 2009; David *et al*. 2010; Kurt-Gür *et al*. 2018). For example, overexpression of the *Arabidopsis* formate dehydrogenase in chloroplasts enhances formaldehyde uptake and resistance in tobacco (Wang *et al*. 2018). The *GhFDH* gene expression was upregulated under copper toxicity, which plays a vital role in the metal detoxification process (Kurt-Gür *et al*. 2018). However, there have been a few studies on the function of FDH genes in response to Al stress.

Mitochondrial respiration holds a critical function in regulating OAs metabolism and maintaining redox equilibrium. Therefore, metabolic engineering has been extensively researched in transgenic plant breeding (Ryan *et al*. 2011). For instance, genes encoding citrate synthase and malate dehydrogenase have been transferred into alfalfa (*Medicago sativa*) (Tesfaye *et al*. 2001; Deng *et al*. 2009) and tobacco (*Nicotiana tabacum*) (Wang *et al*. 2010). The coding genes related to oxidative stress such as manganese superoxide dismutase, dehydroascorbic acid reductase, peroxidase and glutathione S-transferase have also been transferred into plants (Ezaki *et al*. 2000; Basu *et al*. 2001; Dmitriev *et al*. 2016). It provides technical support for the creation of new germplasm resources resistant to Al in tobacco and alfalfa, and the cultivation of new varieties resistant to Al. *VuFDH* overexpression has recently been demonstrated to increase Al tolerance, most likely due to its decreased Al-induced formate production in tobacco (Lou *et al*. 2016a, b). Likewise, *VuAAE3* plays a critical role in Al tolerance mechanisms through its function as oxalyl-CoA synthetase (Lou *et al*. 2016a, b). Additionally, Zhou *et al*. (2018) identified that *GmME1*, a cytosolic NADP-malic enzyme, is implicated in the organic acid pool and confers higher Al resistance by increasing internal malate and citrate concentrations and their external efflux (Zhou *et al*. 2018). These studies suggest that metabolic change is an internal tolerance mechanistic response to Al stress.

TBS is a variety with a strong tolerance to Al by secreting citrate (Wei *et al*. 2020). The function of GmFDH of TBS in formate catabolism and Al tolerance in roots has not been investigated. Under Al stress, we revealed that *GmFDH* was upregulated and caused formate accumulation in TBS root tips. Exogenous formate treatment inhibited root elongation and induced *GmFDH* expression. Consistently, *GmFDH* overexpression in tobacco increased Al tolerance. Moreover, *GmFDH* overexpression enhanced *NtMATE* and *NtALS3* expression in tobacco roots. Our study may provide a gene to improve plant Al tolerance through biotechnology.

Materials and methods

Plant materials and growth conditions

TBS seeds were soaked in 75% ethanol for 1 min, and washed in sterile water thrice, 1 min for each of the first two times, and 10 min for the third time. Then it was soaked in 0.15% $HgCl_2$ twice for 15 min each time for surface sterilization, washed with sterile water 3–4 times, finally soaked for 30 min and germinated in the dark at 25°C. The seedlings were cultured in a tissue culture room with a temperature of 27/22°C and a light time of 14-h light / 10-h dark (200 μmol photons m^{-2} s^{-1}) (Wei *et al*. 2020). After soaking and sterilizing, the tobacco seeds were germinated in 1/2 Murashige and Skoog (MS) medium in darkness and grown in a controlled environment at a day/night temperature of 25/20°C, with 14 h of light (200 μmol photons m^{-2} s^{-1}).

GmFDH gene cloning and bioinformatics analysis

The primers were designed according to the coding regions of *GmFDH*. The primer sequences used for vector construction are listed in table 1 in electronic supplementary material at http://www.ias.ac.in/jgenet/. RT-PCR was used to obtain the PCR product of *GmFDH* gene, which was then sequenced by the Beijing Genomics Institute (BGI). The physicochemical property of GmFDH protein was predicted using ExPASY ProtParam tool server (https://web.expasy.org/protparam/). The SMART (http://smart.embl-heidelberg.de/) and TMHMM (http://www.cbs.dtu.dk/services/TMHMM) tools were used to predict the functional domains and transmembrane domain of GmFDH protein. Amino acid sequences were compared based on genome database, ClustalX sequences with higher homology were compared, and the evolutionary tree was constructed with MEGA X.

Subcellular localization

FDH-GFP primers (table 1 in electroic supplementary material at http://www.ias.ac.in/jgenet/) were designed, and Express II (Vazyme) was used to connect the target gene to the PRTVcGFP vector. The subcellular localization of FDH prediction are provided on the http://www.csbio.sjtu.edu.cn/bioinf/plant-multi/. The vector is transferred into *Arabidopsis* protoplast by protoplast transient transfection technology (Yoo *et al*. 2007). It is incubated for 12 h under the condition of shading and room temperature. Using a pipette, add a small amount of protoplast solution to the slide and gently cover the cover glass from one end to the slide to avoid bubbles as much as possible. Drop a small amount of lens oil on the surface of the cover glass, select GFP excitation, observe the subcellular localization by laser

confocal microscope (LSM710, Leica, Germany), and take photos and records.

Expression analysis of GmFDH in TBS under Al stress

After two weeks of cultivation, the TBS seedlings were pretreated with 0.5 mmol/L $CaCl_2$ (pH 4.5) for 24 h. To analyse the influence of the Al concentration gradient on *GmFDH* expression, the seedlings were transferred and cultured in solutions of 0, 25, 50, 75, and 100 μmol/L $AlCl_3$ (pH 4.3, 0.5 mmol/L $CaCl_2$) for 24 h (Ma *et al*. 2018). To analyse the temporal expression pattern of *GmFDH* in response to Al stress, the seedlings were transferred to a solution of 50 μmol/L $AlCl_3$ (pH 4.3, 0.5 mmol/L $CaCl_2$) for 24 h, and the samples were obtained from the seedlings treated after 3, 6, 9, 12, 15, 18, 21, and 24 h. To analyse *GmFDH* expression pattern in different root segments in response to Al stress, the samples were obtained from seedling roots (sections 0–2, 2–4, and 4–6 cm) after 24 h of treatment with 50 μmol/L $AlCl_3$ solutions. To determine the tissue expression pattern of *GmFDH*, root, stem, leaf, and cotyledon, the samples were collected from seedlings and incubated for 24 h in 50 μmol/L $AlCl_3$ solutions. To analyse the influence of different metal ions on *GmFDH* expression, seven days old seedlings were transferred in solutions of 50 μmol/L $AlCl_3$, 5 μmol/L $CuCl_2$, 50 μmol/L $FeCl_3$, 50 μmol/L $Ga(NO_3)_3$, 50 μmol/L $GrCl_3$, 50 μM $La(NO_3)_3$, and 50 μmol/L $MnCl_2$ for 24 h. To investigate the effect of external formate, the seedlings were exposed to solutions containing 0, 0.25, 0.5, and 1.0 mmol/L formate. Three biological replicates were performed for each treatment.

Total RNA was isolated using the RNAiso Plus kit (Takara, Dalian, China) according to the manufacturer's description. A NanoDrop 2000 spectrophotometer (Thermo, Waltham, USA) was used to measure the total RNA concentration. After DNase treatment, 1 μg total RNA was used as a template for each cDNA synthesis using a PrimeScript RT reagent kit (Takara, Dalian, China). RT-PCR was performed according to our previous work (Wei *et al*. 2020). The *40srRNA* gene (XM_0035498336.4) was used as an endogenous control for RT-qPCR. The primers used are given in table 1 in electronic supplementary material.

Detection of FDH activity and formate content in roots of TBS

Two-week-old TBS seedlings were treated with 0.5 mmol/L $CaCl_2$ and 50 μmol/L $AlCl_3$ (pH 4.5) for 24 h. FDH activity and formate content in root tips were measured using plant formate dehydrogenase ELISA kit and plant formate ELISA kit (SinoBestBio, Beijing, China) according to the instructions. The optical density (OD) at 450 nm was read using a microtiter plate reader within 15 min. The standard curve was constructed by plotting the average OD (450 nm) of each of the six standard concentrations (0, 2, 4, 8, 16, and 32 U/mL for plant formate dehydrogenase ELISA kit and 0, 20, 40, 80, 160, and 320 ng/mL in plant formate ELISA kit) on the vertical (y) axis against the corresponding concentration on the horizontal (x) axis.

Heterologous expression of GmFDH in tobacco

GmFDH was amplified using primers GmFDH-F-*Xba*I and GmFDH-R-*Sma*I (table 1 in electronic supplementary material). The amplifications were cloned into a pMD19-T vector (TAKARA, Beijing, China) and were subsequently transformed into *E. coli* DH5α. Positive colonies were detected by colony PCR, and *GmFDH* was subcloned into pBI121-*eGFP* by *Xba*I and *Sma*I digestion. Positive clones were detected by colony PCR, and pBI121-*GmFDH-eGFP* was sequenced by BGI. The expression vectors were transformed into LBA4404 using a freeze-thawing method and were selected to transfect tobacco through the leaf-disc method.

To screen the transgenic-positive plants, tobacco transfected with pBI121-*GmFDH-eGFP* was grown in 1/2 MS culture medium. All the tobacco plants were selected for DNA isolation in the leaf using Plant DNA isolation reagents (Takara, Beijing, China), and PCR amplification was performed with DNA as templates and primers FDH-F and FDH-R (table 1 in electronic supplementary material). To detect the pBI121-*GmFDH-eGFP* expression, RNA and protein samples were isolated from positive tobacco in DNA and RNA levels, respectively, using RNAiso reagents (TAKARA, Beijing, China) and Plant Protein Extraction kit (Solarbio, Beijing, China). The RNA samples were reverse transcribed using PrimeScript™ RT reagent kit with gDNA Eraser (Perfect Real Time) (Takara, Beijing, China) and amplified using FDH-F and FDH-R (table 1 in electronic supplementary material). Subsequently, the protein samples were used for western blot with primary antibody against GFP (AF5066, Beyotime, Shanghai, China).

Al resistance analysis in transgenic tobacco

Two weeks old transgenic and wild-type seedling tobacco of uniform size were pretreated with 0.5 mmol/L $CaCl_2$ (pH 4.5) for 24 h and then treated with 0 (control) and 50 μmol/L $AlCl_3$ for 48 h. Each treatment had four biological replicates and root tissues from 20 seedlings. The RRG, Evans blue, Chromazurine S, Haematoxylin Staining and Morin staining were used to measure the effect of $AlCl_3$ treatment as previously described (Jiang *et al*. 2018). Further, citrate exudation from roots was detected using a citrate assay kit (Solarbio, cat nos. BC2155) according to the manufacturer's instructions.

To detect Al content in root tips, seedlings of wild type and transgenic tobacco, containing three biological replicates for each with five tobacco plants, were treated as described above. Roots excised from wild type and transgenic tobacco were placed in 15 mL tubes and extracted with 10 mL of 2 mol/L HCl. After shaking the sample tubes for 24 h, Al concentrations in the extracts were determined using a Microwave Plasma Atomic Emission Spectrometer (4210 MP-AES, Agilent Technologies).

Measurement of POD and SOD activities, MDA and H_2O_2 contents in transgenic tobacco

The seedlings of wild-type and transgenic tobacco were treated with 50 μmol/L $AlCl_3$ (pH 4.5) for 24 h. The experiment was three replicates with five strains per replicate. The activities of superoxide dismutase (SOD) and peroxidase (POD), the content of malondialdehyde (MDA) and hydrogen peroxide (H_2O_2) were determined according to the instruction of antioxidant enzyme assays kits (Solarbio, cat nos. BC0175, BC0095, BC0025, BC3595) (Jiang *et al*. 2018). In brief, root apex (0.1 g) of transgenic tobacco and wild type with or without Al treatment were harvested and ground in liquid nitrogen. Subsequently, the extraction was centrifuged at 8000 g for 10 min at 4°C, and the supernatant was used to determine the enzyme activity and MDA content using a spectrometer.

Statistical analysis

All data are expressed as mean ± standard error of mean (SEM). One-way ANOVA, followed by a two-sided Student's *t*-test, was used to compare the significance. Statistical significance was set to $P < 0.05$. Statistical analyses of data were performed using SPSS 22.0.

Results

GmFDH gene cloning and sequence analysis

The full-length CDS primer of *GmFDH* gene was designed according to the soybean genome database. Using the root tip cDNA of TBS as the template, expand with the same size as the target gene were amplified by PCR using primer STAR. The online tool ProtParam (https://web.expasy.org/protparam/) analysis showed that the GmFDH protein was encoding 375 amino acids with an MW of 41.3 kDa. The NCBI database was used to store the sequencing data (accession number: MT793648). The Functional domain (https://www.ncbi.nlm.nih.gov/Structure/cdd/wrpsb.cgi) analysis showed that GmFDH is a PLN03139 family protein (figure 1a in electronic supplementary material). TMHMM Server v.2.0 online software (https://services.healthtech.dtu.dk/service.php?TMHMM-2.0) predicted the transmembrane domain, indicating that GmFDH lacks a transmembrane domain (figure 1b in electronic supplementary material). Secondary structure (https://npsa-prabi.ibcp.fr/cgi-bin/npsa_automat.pl?page=npsa_sopma.html) prediction for secondary structure revealed that GmFDH contained 42.67% α-helix, 9.07% β-turn, 31.47% random coil, and 16.80% extended chain (figure 1c in electronic supplementary material). In addition, the three-dimensional (3D) structure was successfully analysed using tertiary structure (https://www.rcsb.org/) software (figure 1d in electronic supplementary material). Besides, phylogenetic trees revealed that TBS GmFDH protein was most closely clustered with that of wild soybean (*Glycine soja*) (figure 1).

GmFDH is a chloroplast protein

PRTVcGFP is a transient expression vector containing GFP tags, which can see green fluorescence at specific wavelengths and are often used for subcellular localization. As can be seen from figure 2, the green fluorescence mainly appeared in the chloroplast, so GmFDH was located in the chloroplast.

Expression patterns of GmFDH under Al stress

To investigate the expression patterns of *GmFDH* response to acidic Al stresses, the qRT-PCR was used to analyse the expression levels of GmFDH under $AlCl_3$ treatments designed with concentration gradients and time gradients. In a dose-response experiment, *GmFDH* exhibited various responses to different metal treatments, and the expression was the highest under Al stress (figure 3a). Moreover, *GmFDH* was significantly induced when exposed to various Al concentrations and expressed at the highest level when treated with 25 μmol/L $AlCl_3$ (figure 3b). The Al-induced expression of *GmFDH* was found to increase rapidly within 12 h of exposure to 50 μmol/L (figure 3c). The qRT-PCR result showed that *GmFDH* is mainly expressed in the roots (figure 3d). In addition, the highest level of *GmFDH* expression was observed in the 2–4 cm zones of the root measured from the tip (figure 3e). To test the effect of formate on *GmFDH* expression, TBS roots were treated with different formate concentrations. The findings indicated that the *GmFDH* expression increased as the formate concentration increased (figure 3f).

Root FDH activity and formate contents are increased by Al and time

To further verify the involvement of *GmFDH* in Al resistance, we determined the FDH activity and formate content in root tips of TBS under Al stress. Consequently, FDH activity significantly increased as pH decreased and Al

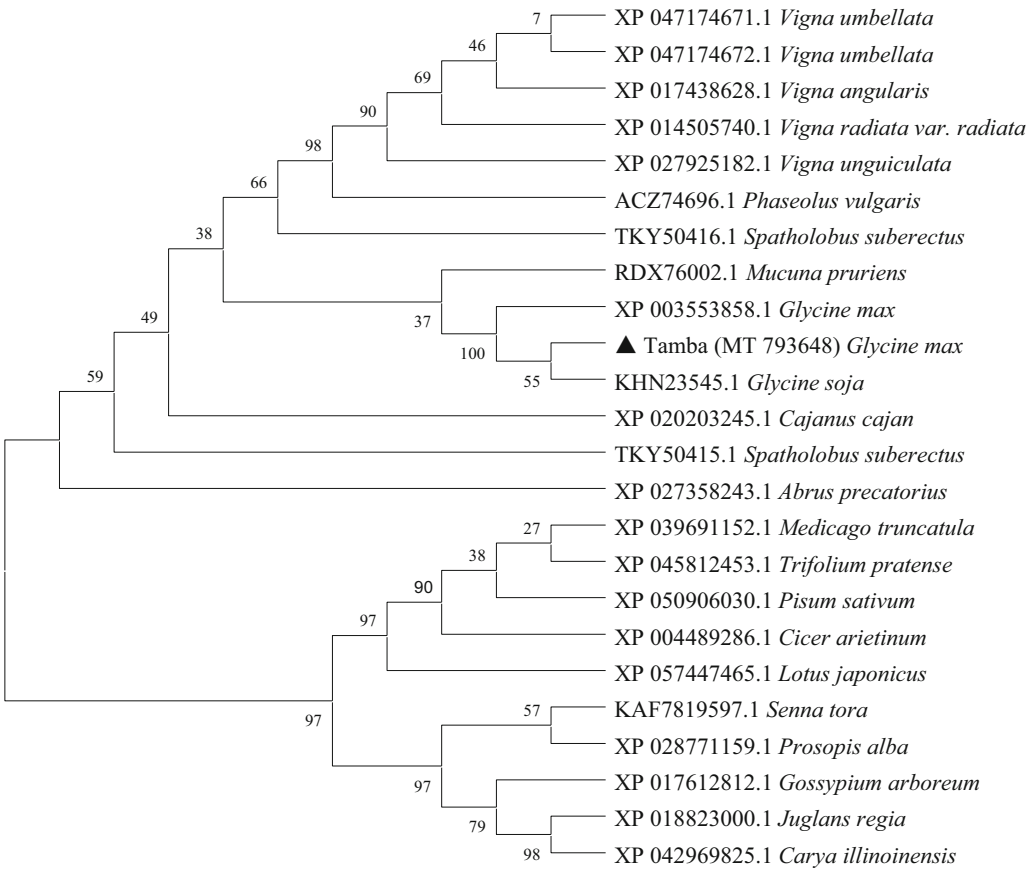

Figure 1. Homology analysis of GmFDH and other FDH proteins. All the available amino acid sequences and the accession numbers of FDH proteins were obtained from NCBI databases (https://www.ncbi.nlm.nih.gov/). The homology tree was produced using MEGA X alignments. The accession numbers of FDH proteins are shown in parentheses. Evolutionary analysis was conducted by maximum likelihood method.

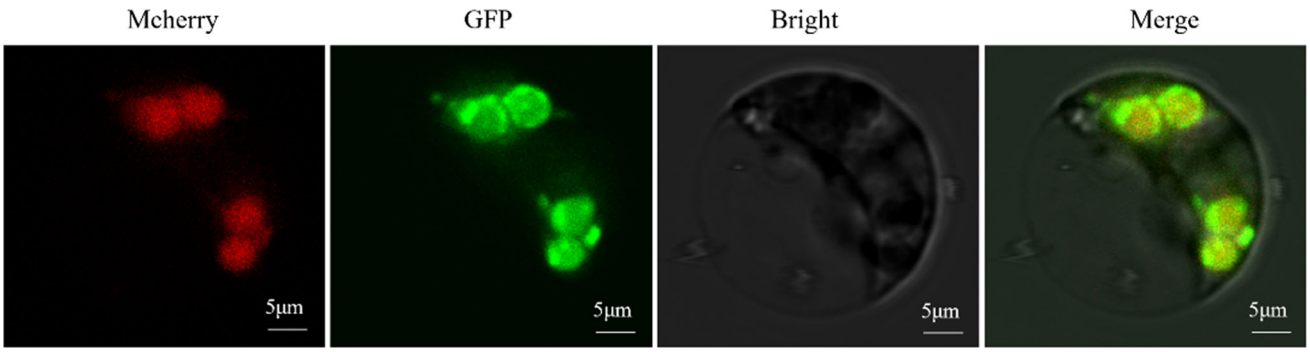

Figure 2. Subcellular localization of GmFDH in *A. thaliana* protoplasts. Constructs expressing GmFDH–GFP fusion protein were transiently expressed in *A. thaliana* protoplasts. Red colour indicates autofluorescence emitted by chloroplasts and green light indicates chloroplast location. Scale bar: 5 μm.

concentrations increased (figure 4, a&b). FDH activity increased with 50 μmol/L $AlCl_3$ treatment time and peaked at 0.5 mmol/L external formate for 24 h (figure 4, c&d). Moreover, formate content in root tips significantly increased as pH decreased and Al concentration increased (figure 4, e&f). The secretion of formate from root tips was increased after treatment with 50 μmol/L $AlCl_3$ and reached the highest level after treatment with 0.5 mmol/L external formate for 24 h (figure 4, g&h). The results indicated that Al stress remarkably affected formate accumulation in TBS root tips, and Al-induced formate accumulation was a response to Al stress. In addition, Al content in root tips was increased as Al concentration (figure 5a) and duration of 50 μmol/L $AlCl_3$ treatment increased (figure 5b). Al concentrations reached the highest level in root tips treated with 0.5 mmol/L external formate for 24 h (figure 5c).

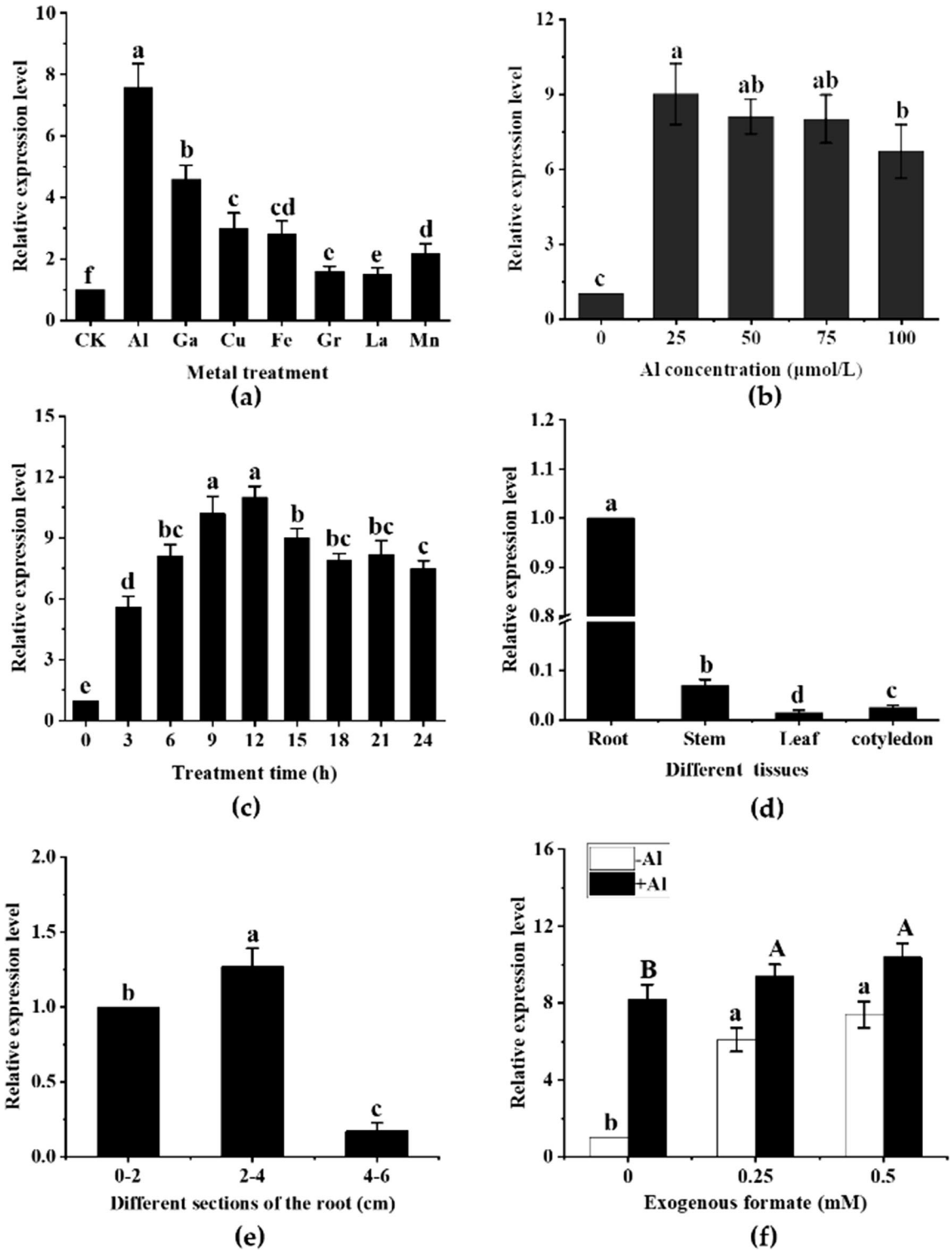

Figure 3. Expression pattern analysis of *GmFDH* gene in TBS. (a) Relative expression level of *GmFDH* treated with different metal ions for 24 h. (b) Relative expression level of *GmFDH* treated with various $AlCl_3$ concentrations for 24 h. (c) Relative expression level of *GmFDH* treated with 50 μmol/L $AlCl_3$ during different treatment times. (d) Tissue expression pattern of *GmFDH*. (e) Relative expression level of *GmFDH* in root sections. (f) Effect of exogenous formate on *GmFDH* expression. Different letters above columns indicate significance at $P < 0.05$. Values are means ± SD ($n = 3$).

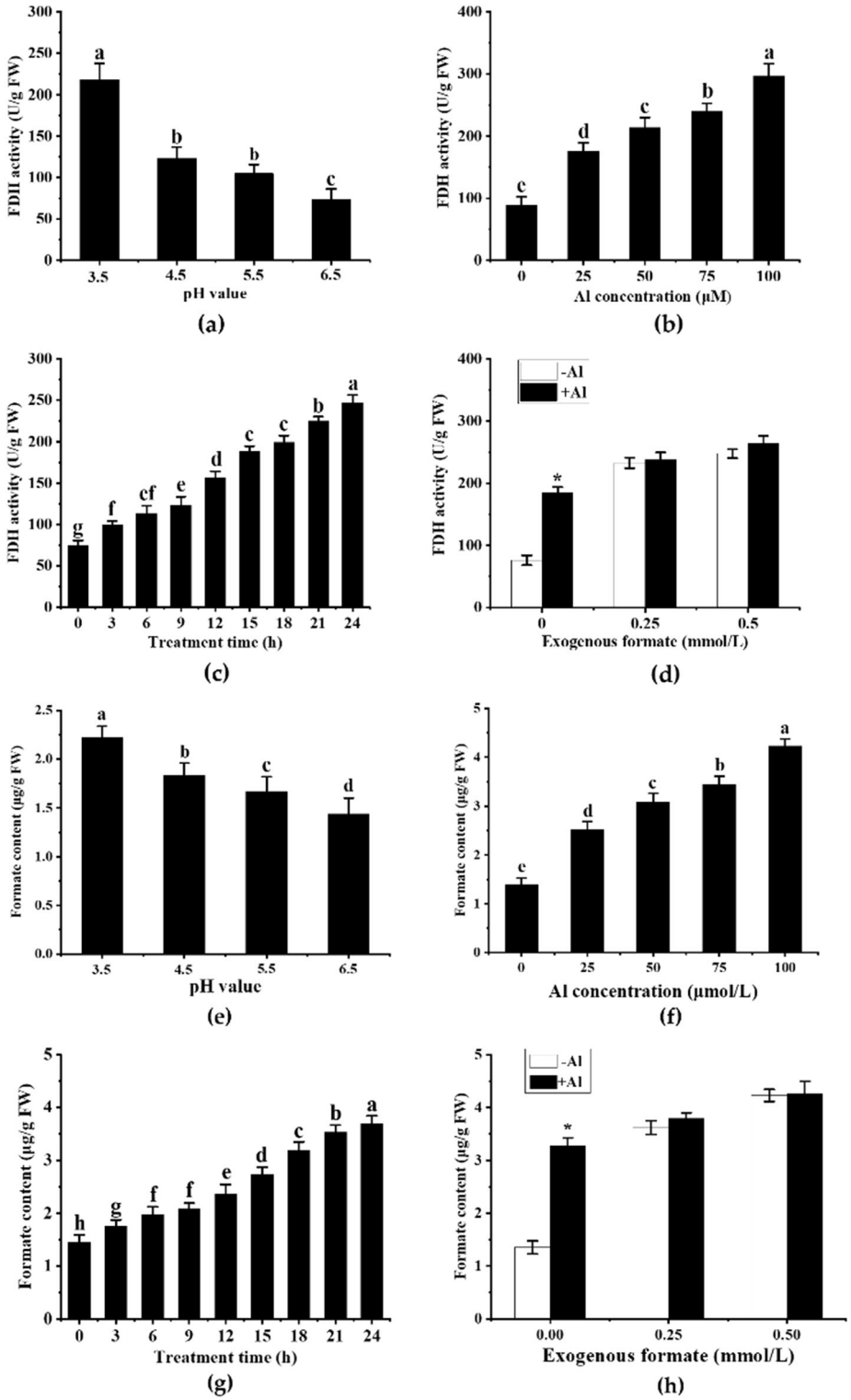

Figure 4. The effect of H^+ stress and Al^{3+} stress on FDH activity and FDH content in TBS root tips. (a) FDH activity in TBS root tips treated at different acidic levels (pH 3.5–6.5) for 24 h. (b) FDH activity in TBS root tips treated with various $AlCl_3$ concentrations for 24 h. (c) FDH activity in TBS root tips treated with 50 μmol/L $AlCl_3$ during different treatment times. (d) FDH activity in TBS root tips treated with exogenous formate for 24 h in $AlCl_3$ solution. (e) FDH content in TBS root tips treated at different acidic levels (pH 3.5–6.5) for 24 h. (f) FDH content in TBS root tips treated with various $AlCl_3$ concentrations for 24 h. (g) FDH content in TBS root tips treated with 50 μmol/L $AlCl_3$ during different treatment times. (h) FDH content in TBS root tips treated with exogenous formate for 24 h in $AlCl_3$ solution. Data are expressed as mean with ± SD (n = 3). Different letters above columns indicate significance at $P < 0.05$. The asterisk indicates significant differences between treatment and control.

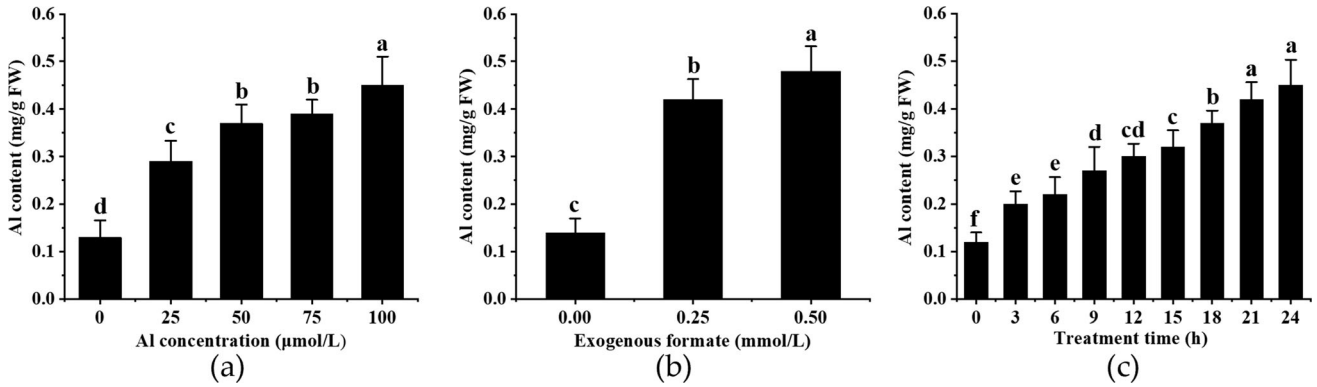

Figure 5. The effect of Al^{3+} stress on Al content in TBS root tips. (a) Al content in TBS root tips treated with various $AlCl_3$ concentrations for 24 h. (b) Al content in TBS root tips treated with 50 μmol/L $AlCl_3$ during different treatment times. (c) Al content in TBS root tips treated with exogenous formate for 24 h in 50 μmol/L $AlCl_3$ solution. Data are expressed as mean with ± SD (n=3). Different letters above columns indicate significance at $P < 0.05$.

Cloning of GmFDH and overexpression of GmFDH in tobacco

To evaluate the role of *GmFDH* in Al stress response, a 35::GmFDH::GFP construct was introduced and transformed into tobacco leaves using *Agrobacterium tumefaciens* strain GV3101 (figure 6a). Fourteen transgenic lines underwent molecular identification to obtain transgenic tobacco plants. The PCR products of a specific band of 1128 bp were detected in different *GmFDH* transgenic lines (figure 6b). The RT-PCR was performed to measure the mRNA levels of *GmFDH* in transgenic lines and wild type, indicating that GmFDH-5, GmFDH-6, and GmFDH-13 had higher transcription levels than other transgenic lines (figure 6c). The western blot was performed to detect the expression level of label protein GFP protein (figure 6d). The qRT-PCR was performed to measure relative expression levels of *GmFDH* in transgenic lines and wild type, indicating that GmFDH-5, GmFDH-6, and GmFDH-13 had higher expression than wild type (figure 6e).

Heterologous expression of GmFDH enhanced Al tolerance in tobacco

To investigate the responses of *GmFDH* transgenic lines to Al stress, the tobacco seedlings were exposed to $AlCl_3$ at 0 or 50 μmol/L for five days. The results indicated that the relative root growth (RRG) of transgenic tobacco plants was more than 45% under Al stress at 50 μmol/L, significantly higher than that of wild type (34%) (figure 7, a&b). Moreover, Evans blue, Chromeazurol S and Hematoxylin staining in root tips of tobacco overexpressing GmFDH became lighter than that of wild type, the fluorescence intensity of Morin staining is stronger than that of wild type. The results showed that the integrity of the plasma membrane of transgenic tobacco was less damaged and the accumulation of Al was less (figure 7c). Moreover, malondialdehyde (MDA), hydrogen peroxide (H_2O_2) content in transgenic tobacco tips were significantly lower than wild type (figure 7, d&e). To further analyse the mechanism underlying Al tolerance of the transgenic tobacco, the Al content in root tips of *GmFDH* tobacco plants and WT were determined under Al stress. The results revealed that Al content in *GmFDH* tobacco plants was significantly lower than in wild type (figure 7f). Additionally, superoxide dismutase (SOD) activity, peroxidase (POD) and FDH activities in *GmFDH* tobacco plants were significantly higher than wild type (figure 7, g–i). These results revealed that GmFDH decreased Al content and conferred the tolerance to Al toxicity in transgenic plants.

GmFDH affects Al tolerance independently of NtALS3 or NtMATE expression

To study the regulatory pathway of *GmFDH* under aluminum stress, qRT-PCR was used to quantify two aluminum stress response genes *NtALS3* (aluminum sensitive protein 3) and *NtMATE* (multidrug toxic complex extrusion protein) in tobacco. The results indicated that the relative expression of *NtMATE* and *NtALS3* was not significantly different under Al stress between transgenic tobacco and wild type (figure 8), suggesting that the enhanced Al tolerance of these transgenic plants is not associated with expression of *NtALS3* or *NtMATE*.

GmFDH enhances Al tolerance by increased citrate secretion

The Al-activated release of citrate from root apex is an important Al-tolerance mechanism in tobacco (Deng *et al.* 2009). To further compare the Al tolerance of different tobacco lines, the citrate secretion of root tips was determined under Al stress. The results showed that citrate secretion from roots of GmFDH-5, GmFDH-6, and GmFDH-13 lines was significantly higher than that of wild-

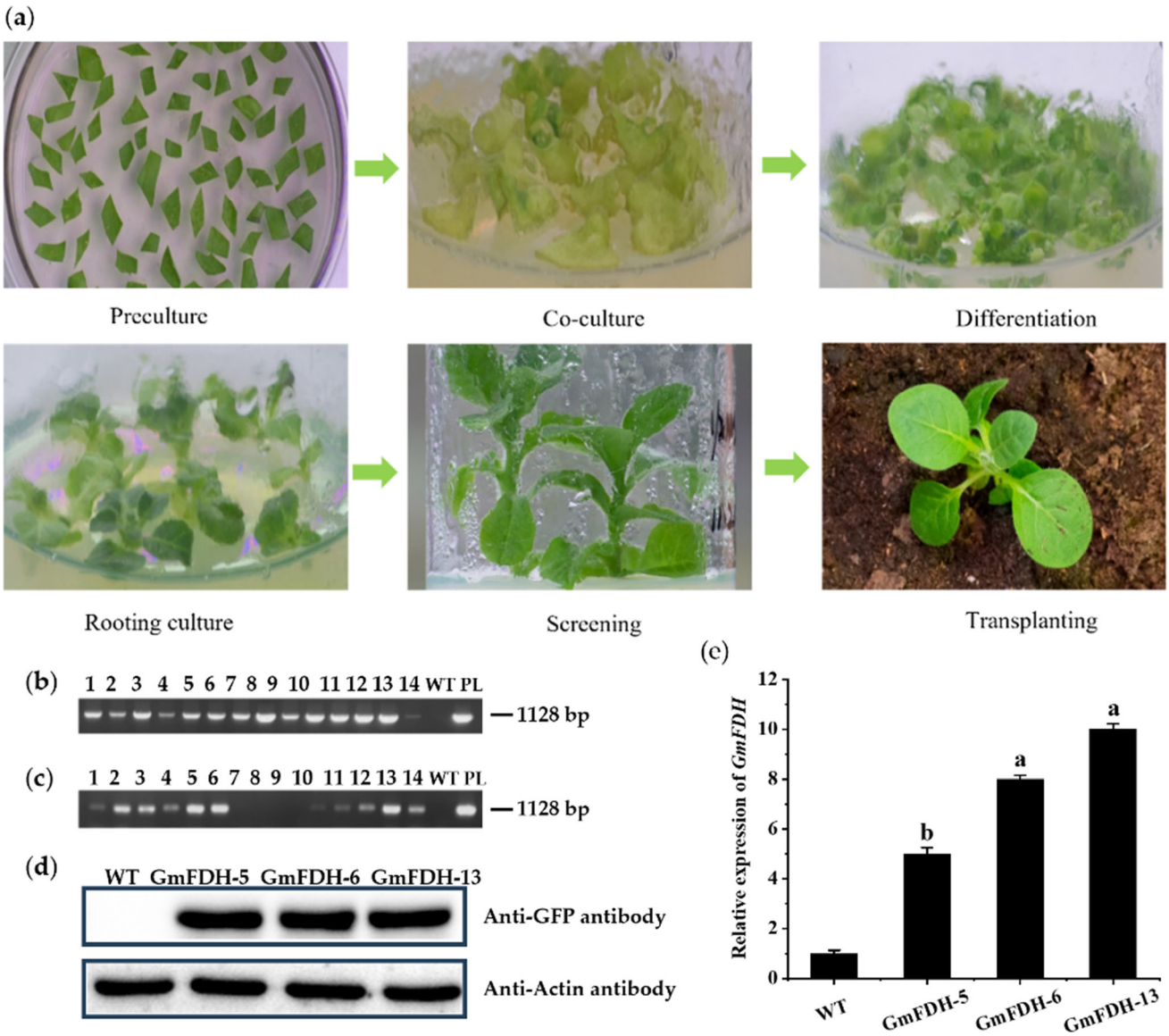

Figure 6. (a) Genetic transformation process of tobacco. (b–d) The overexpression of *GmFDH* gene in transgenic tobacco. (b) Genome detection for integrated *GmFDH* gene. (c) The detection of mRNA level of *GmFDH*. (d) The expression level detection of label protein GFP protein. 1–14, Transgenic tobacco lines; WT, wild-type tobacco; PL, pBI121-*GmFDH-eGFP* plasmid was used as a template. (e) Relative expression levels of *GmFDH* in transgenic tobacco. The expression was determined by RT-PCR and *NtACTIN* was used as an internal control. Data are means ± SD (n = 3).

type plants (figure 9a). Moreover, citrate synthase activity is consistent with citrate secretion results (figure 9b). These results suggest that the increased citrate synthase activity may be the reason for the increased citrate secretion of tobacco overexpressing *GmFDH* under Al stress.

Discussion

Al stress is one of the most limiting factors for plant growth and crop yield in acidic soils. Finding new Al tolerance genes and elucidating their roles is the current challenge. FDH's function as a universal stress protein has been demonstrated to involve plant responses to abiotic and biotic stresses such as chilling, drought, iron deficiency, hypoxia, pathogen, and wounding (Choi *et al*. 2014). Here, *GmFDH* gene encoding a formate dehydrogenase was isolated from the Al-tolerant genotype of TBS, which was remarkably upregulated in roots by Al stress and exogenous formate in a dose-dependent manner (figure 3). A similar result was observed in VuFDH protein, which confers tolerance to low pH and Al stress due to decreased formate production in the transgenic tobacco lines (Lou *et al.* 2014). Therefore, *GmFDH* might function as a formate dehydrogenase and regulate plant tolerance to Al stress.

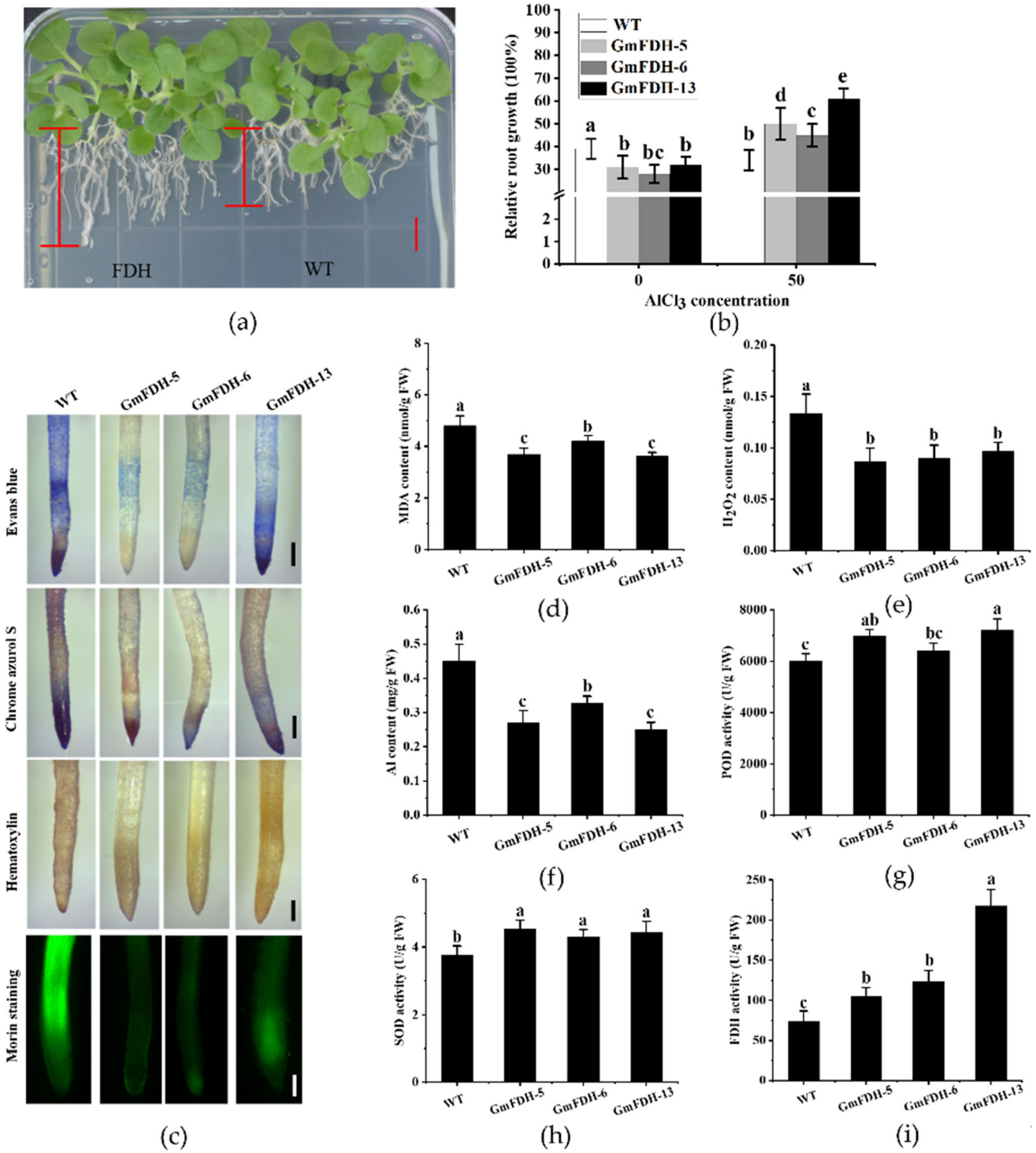

Figure 7. (a) Representative seedlings showing difference in $AlCl_3$ sensitivity between the wild-type and the overexpression lines. Seedlings were grown in the 1/2 MS with 50 μmol/L $AlCl_3$ for seven days. Relative root elongation between wild-type and the transgenic lines grown as described in figure 9a. Data are means ± SD (n = 15). Scale bar: 1 cm. (b–i) Functional assessment in tobacco with the overexpression of *GmFDH* gene. (b) RRG of tobacco treated with 50 μmol/L $AlCl_3$ for seven days. (c) Evans blue, Chromazurol S, and Hematoxylin staining Morin staining of root tips in wild type and transgenic tobacco under 50 μmol/L $AlCl_3$ stress. Scale bar: 1 cm. (d) MDA content, (e) H_2O_2 content, and (f) Al content in wild type and the transgenic tobacco root tips under 50 μmol/L $AlCl_3$ stress for 24 h. (g) POD activity, (h) SOD activity, and (i) FDH activity in wild type and the transgenic tobacco root tips treated with 50 μmol/L $AlCl_3$ for 24 h. Data are expressed as mean with ± SD (n=3). Different letters indicate significant differences between treatments at $P< 0.05$.

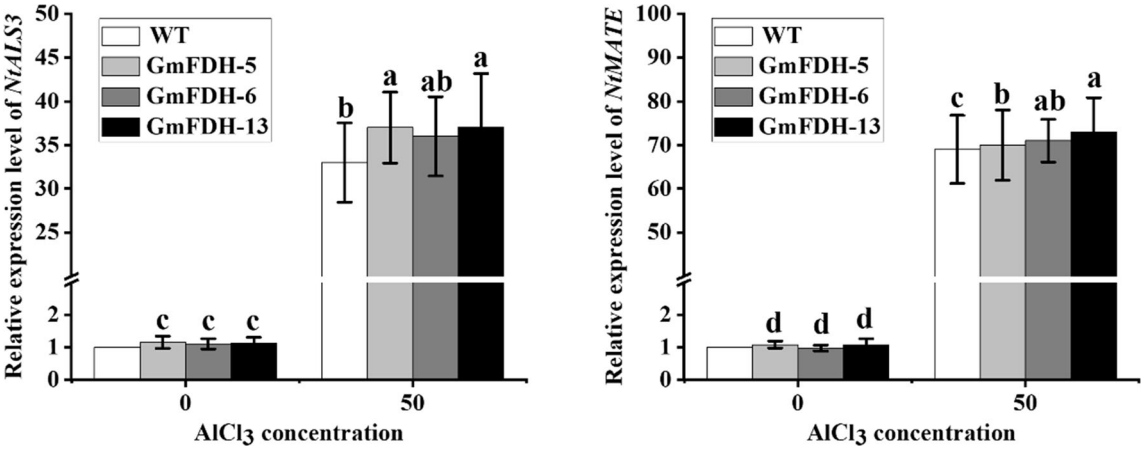

Figure 8. The effect of Al stress on Al-tolerance gene expression in tobacco. (a) Relative expression of *NtALS3* and (b) *NtMATE* of tobacco root tips treated with various $AlCl_3$ concentrations for 24 h. The tobacco lines were exposed to 1:30 strength Hoagland nutrient solution containing 0 or 50 μmol/L $AlCl_3$ for 24 h. The expression was determined by RT-PCR and *NtACTIN* was used as an internal control. Data are means ± SD (n = 3).

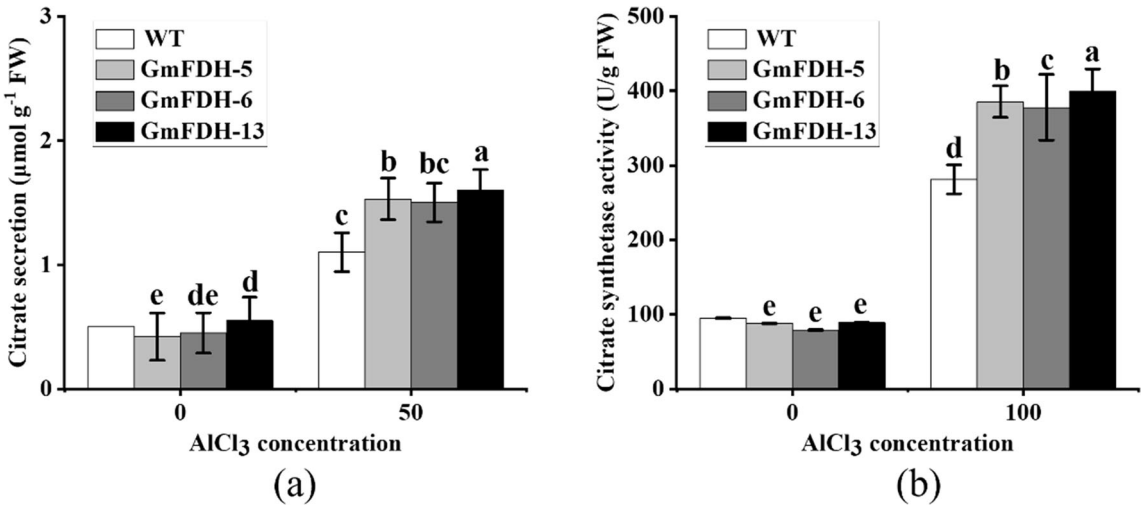

Figure 9. The effect of Al stress on citrate secretion in tobacco. (a) Citrate secretion and (b) citrate synthase activity of tobacco root tips treated with 50 μmol/L $AlCl_3$ for 24 h. Data are expressed as mean with ± SD (n=3). Different letters above columns indicate significance at $P < 0.05$.

To further investigate *GmFDH* function in Al tolerance, transgenic tobacco overexpressing *GmFDH* was generated to verify the tolerance of tobacco to Al stress (figure 6). It is well known that root growth inhibition is the main symptom of Al toxicity (Du *et al*. 2020). The RRG has been used to measure Al stress tolerance in many plants, including *Arabidopsis* (Dong *et al*. 2017), sorghum (Kopittke *et al*. 2017), (Wu *et al*. 2017), peanut (Yao *et al*. 2020) and alfalfa (Li *et al*. 2020) tobacco. For example, the RRG of *GsMATE* transgenic *Arabidopsis* lines was significantly greater than that of wild type under Al stress, indicating that *GsMATE* may enhance the Al tolerance of transgenic plants (Ma *et al*. 2018). Our study results indicated that *GmFDH* tobacco plants had higher RRG than wild type (figure 7b), consistent with those of *VuFDH* overexpression in tobacco (Lou *et al*. 2016a, b). Moreover, staining root tips with Evans blue, Chromazurine S, or Hematoxylin is a critical indicator of plant aluminum tolerance (Ribeiro *et al*. 2017). For example, roots overexpressing *GsGIS3* or *GmME1* genes exhibited marginal haematoxylin staining compared to wild type under Al stress, indicating strong Al resistance (Zhou *et al*. 2018; Liu *et al*. 2020). Evans blue staining revealed that roots overexpressing *GmFDH* have slighter damage than wild type, consistent with RRG in tobacco. Similar results were obtained with Chromazurine S and Haematoxylin staining (figure 7c). These results provide additional evidence that *GmFDH* overexpression confers tolerance to Al stress in tobacco.

Previous studies have stated that ROS accumulation in plants under Al stress is the primary reason for oxidative stress and the decisive factor that inhibits root elongation (Giannakoula *et al*. 2010). MDA content in the roots of

GmFDH tobacco plants is rather lower than that in the wild type (figure 7d). Similarly, H_2O_2 content in transgenic tobacco plants was significantly lower than those in wild type under 50 μmol/L $AlCl_3$ stress (figure 7e). Additionally, MDA injures membrane function and determines the degree of damage to plants, which decreases as Al concentrations decrease (Zhang *et al*. 2018). As shown in figure 9d, the Al content was significantly lower in the root tips of *GmFDH* tobacco plants than that of wild-type plants. Wu *et al*. (2017) also demonstrated that overexpression of a peroxidase gene (*AtPrx64*) in tobacco reduced the accumulation of Al, H_2O_2, and MDA in the roots, implying that overexpression of the *AtPrx64* gene might enhance the tolerance of tobacco to Al stress (Wu *et al*. 2017). These results further support that *GmFDH* enhances Al tolerance in tobacco.

Plants accumulate reactive oxygen species (ROS) in response to Al toxicity, causing damage to DNA, proteins, and lipids, resulting in serious cell damage and even cell death (Sun *et al*. 2017). To avoid Al-triggered oxidative stresses. Plants have evolved the ability to remove reactive oxygen species, reducing ROS production and weakening lipid peroxidation (Wei *et al*. 2021). For instance, overexpression of the alternative oxidase gene alters the respiratory capacity and response to oxidative stress in tobacco cells, thereby enhancing Al toxicity tolerance (Panda *et al*. 2013). Recently, Du *et al*. (2020) demonstrated that overexpression of *ZmAT6* in maize and *Arabidopsis* confer Al tolerance by increasing the activity of several enzymes within the antioxidant system (Du *et al*. 2020). In this study, increased antioxidant enzyme activity was observed in the root tips of *GmFDH* tobacco plants, suggesting that overexpression of *GmFDH* gene might enhance the antioxidant enzyme activity in response to Al stress. However, the reason for *GmFDH*-induced increase in antioxidant enzyme activity in tobacco plants is still unknown and warrants further investigation.

OAs secretion is an important strategy for plants to respond to Al stress (Yang *et al*. 2011; Guo *et al*. 2013; Wu *et al*. 2014). Increasing evidence shows that Al-induced secretion of OAs may be related to anion channels, internal concentrations of OAs, and plasma membrane H^+-ATPase (Yang *et al*. 2013). For instance, *GmME1* encodes a cytosolic malic enzyme that confers higher Al resistance by increasing internal malate and citrate concentrations and external efflux (Zhou *et al*. 2018). Sun *et al*. (2020) found that the level of *MsCS* transcript was higher in Al tolerant cultivar than Al sensitive cultivar, and the activity of citrate synthase (CS) affected Al resistance via citrate concentration and exudation in alfalfa cultivar (Sun *et al*. 2020). In the present study, the citrate secretion of transgenic tobacco root tips was significantly higher than that of wild type (figure 9a), indicating that overexpression of the *GmFDH* gene promoted citrate secretion, which might be a fundamental reason for enhanced Al tolerance of *GmFDH* tobacco. Previous studies showed that *NtSTOP1* acts as a central regulator of Al-induced signalling by modulating the expression of Al-tolerance genes such as citrate transporting *NtMATE* and *NtALS3* (Ito *et al*. 2019). However, the expression of *NtMATE* and *NtALS3* was not significantly different under Al stress between transgenic tobacco and wild type (figure 8), consistent with *VuAAE3* or *VuFDH* gene overexpression results in tobacco. Interestingly, citrate synthase activity is higher in transgenic tobacco than in wild type, which might be the reason for increased citrate secretion. Therefore, our results indicated that *GmFDH* overexpression promotes citrate secretion by activating citrate synthase activity.

In summary, we characterized *GmFDH*, and showed that it is a formate dehydrogenase that mediates oxidation of the formate that is produced in conditions of Al stresses. To the best of our knowledge, this is the first report of the increased Al tolerance of *GmFDH* overexpression lines is likely attributable to enhanced activities of antioxidant enzymes and promoting citrate secretion. We have shown that tobacco plants overexpressing *GmFDH* display an increased ability to tolerate of Al stress. In this study, the function of *GmFDH* gene in tobacco Al resistance was studied by haematoxylin staining (Lou *et al*. 2014), citric acid secretion determination, subcellular localization, bioinformatics analysis, and other methods in tobacco overexpressing *GmFDH* gene under Al stress, it plays an important role in the process of plant Al resistance, provides genetic resources for cultivating plant Al resistance varieties, and provides a scientific basis for further elucidating the mechanism of plant Al resistance. So as to provide the scientific basis for further clarifying the mechanism of plant Al resistance.

Acknowledgements

This research was funded by the National 973 Project of China (2014CB138701).

Authors' contributions

Conceptualization and writing: YX and YW; analysis: YX, YW and RH; investigation: RH, SY and LL; supervision: YY and JC.

References

Ambard-Bretteville F., Sorin C., Rébeillé F., Hourton-Cabassa C. and des Colas Francs-Small C. 2003 Repression of formate dehydrogenase in Solanum tuberosum increases steady-state levels of formate and accelerates the accumulation of proline in response to osmotic stress. *Plant Mol. Biol.* **52**, 1153–1168.

An Y., Zhou P., Xiao Q. and Shi D. 2014 Effects of foliar application of organic acids on alleviation of aluminum toxicity in alfalfa. *J. Soil Sci. Plant Nut.* **177**, 421–430.

Andreadeli A., Flemetakis E., Axarli I., Dimou M., Udvardi M. K., Katinakis P. *et al*. 2009 Cloning and characterization of Lotus japonicus formate dehydrogenase: a possible correlation with hypoxia. *Biochim. Biophys. Acta* **1794**, 976–984.

Basu U., Good A. G. and Taylor G. J. 2001 Transgenic Brassica napus plants overexpressing aluminium-induced mitochondrial

manganese superoxide dismutase cDNA are resistant to aluminium. *Plant Cell Environ.* **24**, 1278–1269.
Choi D. S., Kim N. H. and Hwang B. K. 2014 Pepper mitochondrial FORMATE DEHYDROGENASE1 regulates cell death and defense responses against bacterial pathogens. *Plant Physiol.* **166**, 1298–1311.
David P., des Colas Francs-Small C., Sévignac M., Thareau V., Macadré C., Langin T. *et al*. 2010 Three highly similar formate dehydrogenase genes located in the vicinity of the B4 resistance gene cluster are differentially expressed under biotic and abiotic stresses in Phaseolus vulgaris. *Theor. Appl. Genet.* **121**, 87–103.
Deng W., Luo K., Li Z., Yang Y., Hu N. and Wu Y. 2009 Overexpression of Citrus junos mitochondrial citrate synthase gene in Nicotiana benthamiana confers aluminum tolerance. *Planta* **230**, 355–365.
Dmitriev A. A., Krasnov G. S., Rozhmina T. A., Kishlyan N. V., Zyablitsin A. V. *et al*. 2016 Glutathione S-transferases and UDP-glycosyltransferases are involved in response to aluminum stress in flax. *Front. Plant Sci.* **7**, 1920.
Dong J., Pineros M. A., Li X., Yang H., Liu Y., Murphy A. S. *et al*. 2017 An Arabidopsis ABC transporter mediates phosphate deficiency-induced remodeling of root architecture by modulating iron homeostasis in roots. *Mol. Plant.* **10**, 244–259.
Du H., Huang Y., Qu M., Li Y., Hu X., Yang W. *et al*. 2020 A maize *ZmAT6* gene confers aluminum tolerance via reactive oxygen species scavenging. *Front. Plant Sci.* **11**, 1016.
Eekhout T., Larsen P. and De Veylder L. 2017 Modification of DNA checkpoints to confer aluminum tolerance. *Trends Plant Sci.* **22**, 102–105.
Ezaki B., Gardner R. C., Ezaki Y. and Matsumoto H. 2000 Expression of aluminum-induced genes in transgenic Arabidopsis plants can ameliorate aluminum stress and/or oxidative stress. *Plant Physiol.* **122**, 657–666.
Giannakoula A., Moustakas M., Syros T. and Yupsanis T. 2010 Aluminum stress induces up-regulation of an efficient antioxidant system in the Al-tolerant maize line but not in the Al-sensitive line. *Environ. Exp. Bot.* **67**, 487–494.
Guo C. L., Chen Q., Zhao X. L., Chen X. Q., Zhao Y., Wang L. *et al*. 2013 Al-enhanced expression and interaction of 14-3-3 protein and plasma membrane H^+-ATPase is related to Al-induced citrate secretion in an Al-resistant black soybean. *Plant Mol. Biol. Rep.* **31**, 1012–1024.
He H., Li Y. and He L. F. 2019 Aluminum toxicity and tolerance in Solanaceae plants. *S. Afr. J. Bot.* **123**, 23–29.
Ito H., Kobayashi Y. *et al*. 2019 Characterization of *NtSTOP1*-regulating genes in tobacco under aluminum stress. *Soil Sci. Plant Nutr.* **65**, 251–258.
Jiang C., Liu L., Li X., Han R., Wei Y. and Yu Y. 2018 Insights into aluminum-tolerance pathways in Stylosanthes as revealed by RNA-Seq analysis. *Sci. Rep.* **8**, 1–9.
Kochian L. V., Piñeros M. A., Liu J. and Magalhaes J. V. 2015 Plant adaptation to acid soils: the molecular basis for crop aluminum resistance. *Annu. Rev. Plant Biol.* **66**, 571–598.
Kopittke P. M., Gianoncelli A., Kourousias G., Green K. and McKenna B. A. 2017 Alleviation of Al toxicity by Si is associated with the formation of Al–Si complexes in root tissues of sorghum. *Front. Plant Sci.* **8**, 2189, https://doi.org/10.3389/fpls.2017.02189.
Kurt-Gür G., Demirci H., Sunulu A. and Ordu E. 2018 Stress response of NAD^+-dependent formate dehydrogenase in Gossypium hirsutum L. grown under copper toxicity. *Environ. Sci. Pollut. Res. Int.* **25**, 31679–31690.
Lei G. J., Yokosho K., Yamaji N., Fujii-Kashino M. and Ma J. F. 2017 Functional characterization of two half-size ABC transporter genes in aluminium-accumulating buckwheat. *New Phytol.* **215**, 1080–1089.
Li J., Su L., Lv A., Li Y., Zhou P. and An Y. 2020 *MsPG1* alleviated aluminum-induced inhibition of root growth by decreasing aluminum accumulation and increasing porosity and extensibility of cell walls in alfalfa (Medicago sativa). *Environ. Exp. Bot.* **175**, 104045.
Liu Y. T., Shi Q. H., Cao H. J., Ma Q. B., Nian H. and Zhang X. X. 2020 Heterologous expression of a Glycine soja C_2H_2 zinc finger gene improves aluminum tolerance in Arabidopsis. *Int. J. Mol. Sci.* **21**, 2754.
Lou G. C., Yang J. M., Xu Q. S., Wei H., Shi S. G. 2014 A retrospective study on endoscopic missing diagnosis of colorectal polyp and its related factors. *Turk. J. Gastroenterol.* **25**, 182–186. https://doi.org/10.5152/tjg.2014.4664
Lou H. Q., Fan W., Xu J. M., Gong Y. L., Jin J. F., Chen W. W. *et al*. 2016a An oxalyl-CoA synthetase is involved in oxalate degradation and aluminum tolerance. *Plant Physiol.* **172**, 1679–1690.
Lou H. Q., Gong Y. L., Fan W., Xu J. M., Liu Y., Cao M. J. *et al*. 2016b A formate dehydrogenase confers tolerance to aluminum and low pH. *Plant Physiol.* **171**, 294–305.
Ma Q., Yi R., Li L., Liang Z., Zeng T., Zhang Y. *et al*. 2018 *GsMATE* encoding a multidrug and toxic compound extrusion transporter enhances aluminum tolerance in Arabidopsis thaliana. *BMC Plant Biol.* **18**, 1–10.
Muhammad N., Zvobgo G. and Zhang G. P. 2019 A review: the beneficial effects and possible mechanisms of aluminum on plant growth in acidic soil. *Front. Plant Sci.* **18**, 1518–1528.
Panda S. K., Sahoo L., Katsuhara M. and Matsumoto H. 2013 Overexpression of alternative oxidase gene confers aluminum tolerance by altering the respiratory capacity and the response to oxidative stress in tobacco cells. *Mol. Biotechnol.* **54**, 551–563.
Riaz M., Yan L., Wu X., Hussain S., Aziz O. and Jiang C. 2018 Mechanisms of organic acids and boron induced tolerance of aluminum toxicity: a review. *Ecotoxicol. Environ. Saf.* **165**, 25–35.
Ribeiro A. P., de Souza W. R., Martins P. K., Vinecky F., Duarte K. E., Basso M. *et al*. 2017 Overexpression of *BdMATE* gene improves aluminum tolerance in Setaria viridis. *Front. Plant Sci.* **8**, 865.
Ryan P. R., Tyerman S. D., Sasaki T., Furuichi T., Yamamoto Y., Zhang W. H. *et al*. 2011 The identification of aluminium-resistance genes provides opportunities for enhancing crop production on acid soils. *J. Exp. Bot.* **62**, 9–20.
Sun C., Liu L., Zhou W., Lu L., Jin C. and Lin X. 2017 Aluminum induces distinct changes in the metabolism of reactive oxygen and nitrogen species in the roots of two wheat genotypes with different aluminum resistance. *J. Agric. Food Chem.* **65**, 9419–9427.
Sun G., Zhu H., Wen S., Liu L., Gou L. and Guo Z. 2020 Citrate synthesis and exudation confer Al resistance in alfalfa (Medicago sativa L.). *Plant Soil.* **449**, 319–329.
Tesfaye M., Temple S. J., Allan D. L., Vance C. P. and Samac D. A. 2001 Overexpression of malate dehydrogenase in transgenic alfalfa enhances organic acid synthesis and confers tolerance to aluminum. *Plant Physiol.* **127**, 1836–1844.
Thomas S. C., Alhasawi A., Auger C., Omri A. and Appanna V. D. 2016 The role of formate in combatting oxidative stress. *Antonie Van Leeuwenhoek* **109**, 263–271.
Wang Q. F., Zhao Y., Yi Q., Li K. Z., Yu Y. X. and Chen L. M. 2010 Overexpression of malate dehydrogenase in transgenic tobacco leaves: enhanced malate synthesis and augmented Al-resistance. *Acta Physiol. Plant.* **32**, 1209–1220.
Wang R., Zeng Z., Guo H., Tan H., Liu A., Zhao Y. *et al*. 2018 Over-expression of the Arabidopsis formate dehydrogenase in chloroplasts enhances formaldehyde uptake and metabolism in transgenic tobacco leaves. *Planta* **247**, 339–354.

Wei Y., Jiang C., Han R., Xie Y., Liu L. and Yu Y. 2020 Plasma membrane proteomic analysis by TMT-PRM provides insight into mechanisms of aluminum resistance in tamba black soybean roots tips. *PeerJ.* **8**, e9312.

Wei Y., Han R., Xie Y., Jiang C. and Yu Y. 2021 Recent advances in understanding mechanisms of plant tolerance and response to aluminum toxicity. *Sustain.-Basel* **13**, 1782.

Wu X., Li R., Shi J., Wang J., Sun Q., Zhang H. *et al*. 2014 Brassica oleracea MATE encodes a citrate transporter and enhances aluminum tolerance in Arabidopsis thaliana. *Plant Cell Physiol.* **55**, 1426–1436.

Wu Y., Yang Z., How J., Xu H., Chen L. and Li K. 2017 Overexpression of a peroxidase gene (*AtPrx64*) of Arabidopsis thaliana in tobacco improves plant's tolerance to aluminum stress. *Plant Mol. Biol.* **95**, 157–168.

Yang X. Y., Yang J. L., Zhou Y., Pineros M. A., Kochian L. V., Li G. X. and Zheng S. J. 2011 A de novo synthesis citrate transporter, Vigna umbellata multidrug and toxic compound extrusion, implicates in Al-activated citrate efflux in rice bean (Vigna umbellata) root apex. *Plant Cell Environ.* **34**, 2138–2148.

Yang L. T., Qi Y. P., Jiang H. X. and Chen L. S. 2013 Roles of organic acid anion secretion in aluminium tolerance of higher plants. *Biomed. Res. Int.*, https://doi.org/10.1155/2013/173682.

Yang J. L., Fan W. and Zheng S. J. 2019 Mechanisms and regulation of aluminum-induced secretion of organic acid anions from plant roots. *J. Zhejiang Univ. Sci. b.* **20**, 513–527.

Yao S., Luo S., Pan C., Xiong W., Xiao D., Wang A. *et al*. 2020 Metacaspase MC1 enhances aluminum-induced programmed cell death of root tip cells in Peanut. *Plant Soil.* **448**, 479–494.

Yokosho K., Yamaji N., Mitani-Ueno N., Shen R. F. and Ma J. F. 2016 An aluminum-inducible *IREG* gene is required for internal detoxification of aluminum in buckwheat. *Plant Cell Physiol.* **57**, 1169–1178.

Yoo S. D., Cho Y. H. and Sheen J. 2007 Arabidopsis mesophyll protoplasts: a versatile cell system for transient gene expression analysis. *Nat. Protoc.* **2**, 1565–1572.

Zhang H., Zheng J., Su H., Xia K., Jian S. and Zhang M. 2018 Molecular cloning and functional characterization of the dehydrin (*IpDHN*) gene from Ipomoea pes-caprae. *Front Plant Sci.* **57**, 1454.

Zhang X., Long Y., Huang J. and Xia J. 2019 Molecular mechanisms for coping with Al toxicity in plants. *Int. J. Mol. Sci.* **20**, 1551.

Zhou Y., Yang Z., Xu Y., Sun H., Sun Z., Lin B. *et al*. 2018 Soybean NADP-malic enzyme functions in malate and citrate metabolism and contributes to their efflux under Al stress. *Front. Plant Sci.* **8**, 2246.

Corresponding editor: Manoj Prasad